

---

# Projection Implicit Q-Learning with Support Constraint for Offline Reinforcement Learning

---

Xinchen Han<sup>1</sup> Hossam Afifi<sup>1</sup> Michel Marot<sup>1</sup>

## Abstract

Offline Reinforcement Learning (RL) faces a critical challenge of extrapolation errors caused by out-of-distribution (OOD) actions. Implicit Q-Learning (IQL) algorithm employs expectile regression to achieve in-sample learning, effectively mitigating the risks associated with OOD actions. However, the fixed hyperparameter in policy evaluation and density-based policy improvement method limit its overall efficiency. In this paper, we propose Proj-IQL, a projective IQL algorithm enhanced with the support constraint. In the policy evaluation phase, Proj-IQL generalizes the one-step approach to a multi-step approach through vector projection, while maintaining in-sample learning and expectile regression framework. In the policy improvement phase, Proj-IQL introduces support constraint that is more aligned with the policy evaluation approach. Furthermore, we theoretically demonstrate that Proj-IQL guarantees monotonic policy improvement and enjoys a progressively more rigorous criterion for superior actions. Empirical results demonstrate the Proj-IQL achieves state-of-the-art performance on D4RL benchmarks, especially in challenging navigation domains.

## 1. Introduction

Offline RL is dedicated to learning policies from static datasets generated by unknown behavior policies, thereby eliminating the need for extensive interactions with the environment (Prudencio et al., 2023; Levine et al., 2020). This data-driven approach has immense potential for real-world applications in high-risk or high-cost domains (Han et al., 2024), bridging the gap between simulated environments and practical deployment. However, while the ability to learn without continuous interactions is a key advantage, it

<sup>1</sup>Samovar, Institut Polytechnique de Paris, Paris, France. Correspondence to: Xinchen Han <xinchen.han@telecom-sudparis.eu>.

*Under Review.*

also introduces significant challenges. One of the most crucial issues is the extrapolation error (Fujimoto et al., 2019), which arises from OOD actions and can lead to severely erroneous value evaluation. These errors propagated through the bootstrapping Bellman operator, can distort value estimates for other state-action pairs. To address this issue, numerous offline RL algorithms have been developed specifically to mitigate this issue in the policy improvement and policy evaluation phases, respectively.

In the policy improvement phase, policy constraint methods restrict the learned policy to remain close to the behavior policy. Behavior Cloning (BC) (Pomerleau, 1991) directly trains the policy to imitate actions within the dataset via supervised learning, while weighted Behavior Cloning (wBC) (Peters & Schaal, 2007; Peng et al., 2019; Nair et al., 2020; Wang et al., 2020) improves upon BC by weighting samples based on different methods. Essentially, wBC methods keep the policy to be close to the behavior policy by Kullback–Leibler (KL) divergence constraint, which is categorized into density constraint methods. However, the constraints in both BC and wBC methods are overly restrictive, thus limiting the performance of policy improvement. In contrast, support constraint methods (Kumar et al., 2019; Wu et al., 2022; Mao et al., 2023; 2024) apply more relaxed constraints to achieve similar policy alignment while allowing for greater policy improvement within the dataset.

In the policy evaluation phase, conservative value learning methods mitigate overestimation issues caused by OOD actions (Kumar et al., 2020; Peng et al., 2023; Kostrikov et al., 2021). Especially, IQL (Kostrikov et al., 2021) employs expectile regression to approximate an upper expectile of the value distribution instead of relying on the traditional maximum operator in Q-Learning. Specifically, IQL alternates between fitting the value function via expectile regression and using it to compute Bellman backups for training the  $Q$ -function. However, IQL has two notable limitations: (1) IQL relies on a fixed conservatism parameter  $\tau$ , requiring extensive tuning across datasets to achieve optimal performance; (2) as a fundamentally one-step (Brandfonbrener et al., 2021) algorithm, IQL restricts the extension for more effective policy improvement.

To overcome these challenges, we propose Projection IQL

with Support Constraint (Proj-IQL). Proj-IQL introduces two key innovations: (1) Proj-IQL replaces the fixed conservatism parameter  $\tau$  with a projection-based adaptive parameter  $\tau_{\text{proj}}(a|s)$ . This approach eliminates the need for dataset-specific fine-tuning and extends IQL to a multi-step algorithm while preserving in-sample learning and the expectile regression framework. (2) Proj-IQL incorporates the support constraint that aligns with its policy evaluation, enabling effective policy improvement while mitigating extrapolation error.

Theoretically, we demonstrate that Proj-IQL is a multi-step offline RL method while preserving the expectile regression framework. Moreover, under the assumption that  $\tau_{\text{proj}}$  is non-decreasing, Proj-IQL provides policy improvement guarantees and enjoys a progressively more rigorous criterion for superior actions.

Experimentally, Proj-IQL achieves state-of-the-art performance on the D4RL benchmarks (Fu et al., 2020), including Gym-MuJoCo-v2 locomotion tasks, AntMaze-v0, and Kitchen-v0 navigation tasks, particularly excelling in challenging “stitching” navigation tasks.

Our key contributions are summarized as follows:

- **1. Proj-IQL Algorithm.** We introduce a projection-based IQL algorithm that integrates multi-step evaluation and support constraint mechanisms, enhancing both policy evaluation and policy improvement.
- **2. Theoretical Guarantee.** We provide theoretical insights demonstrating that Proj-IQL preserves the expectile regression framework, guarantees monotonic policy improvement, and achieves more rigorous criterion for superior actions.
- **3. Empirical Performance.** We evaluate Proj-IQL against other competitive offline RL algorithms on the D4RL benchmark, demonstrating that Proj-IQL achieves state-of-the-art performance.

## 2. Related Work

To more effectively compare and demonstrate the advantages of Proj-IQL, we classify existing offline RL approaches into two main categories: conservative value methods and policy constraint methods.

**Conservative Value Methods** aim to mitigate the overestimation of OOD actions by penalizing overly optimistic value estimates. CQL (Kumar et al., 2020) introduces penalties on the  $Q$ -function for OOD actions, ensuring policy performance while staying close to the behavior policy. Extensions like ACL-QL (Wu et al., 2024) dynamically adjusts penalty term to reduce over-conservatism, and CSVE (Chen et al., 2024) penalizes state value function estimates across

the dataset to enhance generalization. Despite their efficacy in avoiding overestimation, these approaches still face OOD action risk. In-sample learning approaches such as Onestep (Brandfonbrener et al., 2021), IQL (Kostrikov et al., 2021), and IVR (Xu et al., 2023) eliminate the need to estimate  $Q$ -values for OOD actions entirely. Onestep demonstrates strong results with one-step policy improvement but relies on well-covered datasets. IVR introduces an implicit value regularization framework, but Sparse Q-Learning within IVR relies on a restrictive assumption to simplify its optimization objective. IQL leverages the expectile regression framework for value learning, but its hyperparameter  $\tau$  requires careful tuning, which is time-consuming.

**Policy Constraint Methods** enforce closeness between the learned policy and the behavior policy using various metrics such as KL divergence (Nair et al., 2020; Zhang et al., 2021), regularization terms (Fujimoto & Gu, 2021), or CVAE model (Fujimoto et al., 2019; Zhou et al., 2021; Chen et al., 2022), etc. While these density-based methods perform well under moderate suboptimality, they struggle when the dataset predominantly consists of poor-quality data. Support-based approaches relax density constraints to allow greater optimization flexibility. BEAR (Kumar et al., 2019) keep the policy within the support of behavior policy by Maximum Mean Discrepancy (MMD). By contrast, SPOT (Wu et al., 2022) adopts a VAE-based density estimator to explicitly model the support set of behavior policy. Similarly, DASCO (Vuong et al., 2022) employs discriminator scores in Generative Adversarial Networks (GANs). Although these methods achieve strong empirical performance, they lack rigorous policy improvement guarantees, as highlighted by STR (Mao et al., 2023).

Proj-IQL addresses these limitations by providing rigorous policy improvement guarantees. Compared to STR, Proj-IQL progressively tightens the policy evaluation function and raises standards of superior actions in datasets. Moreover, as an in-sample learning algorithm, Proj-IQL avoids the challenges of OOD action estimation, ensuring more reliable and efficient learning.

## 3. Preliminaries

### 3.1. Offline RL

Conventionally, the RL problem is defined as a Markov Decision Process (MDP) (Sutton & Barto, 2018), specified by a tuple  $\mathcal{M} = \langle \mathcal{S}, \mathcal{A}, \mathcal{T}, r, \gamma \rangle$ , where  $\mathcal{S}$  denotes the state space,  $\mathcal{A}$  is the action space,  $\mathcal{T}$  represents the transition function,  $r$  is the reward function, and  $\gamma \in (0, 1)$  denotes the discount factor.

For policy  $\pi(a|s)$ , the  $Q$ -function  $Q^\pi(s, a)$  is defined as the

expectation of cumulative discounted future rewards,

$$Q^\pi(s, a) = \mathbb{E}_{\substack{a_t \sim \pi(\cdot|s_t) \\ s_{t+1} \sim \mathcal{T}(\cdot|s_t, a_t)}} \left[ \sum_{t=0}^{\infty} \gamma^t r(s_t, a_t) \mid s_0 = s, a_0 = a \right]. \quad (1)$$

the value function  $V^\pi(s) = \mathbb{E}_{a \sim \pi} [Q^\pi(s, a)]$ , and the advantage function  $A^\pi(s, a) = Q^\pi(s, a) - V^\pi(s)$ . The  $Q$ -function is updated by minimizing the Temporal Difference (TD) error, shown in the following Eq. (2).

$$L_{\text{TD}}(\theta) = \mathbb{E}_{\mathcal{B}} \left[ [r(s, a) + \gamma \max_{a'} Q_{\hat{\theta}}(s', a') - Q_\theta(s, a)]^2 \right]. \quad (2)$$

where  $\mathcal{B}$  is the replay buffer  $(s, a, s') \sim \mathcal{B}$ . When the state-action space is large, the  $Q$ -function is approximated by neural networks  $Q_\theta(s, a)$  and parameterized by  $\theta$ , and the  $Q_{\hat{\theta}}(s, a)$  represents the target- $Q$  network whose parameters  $\hat{\theta}$  are updated via Polyak averaging.

In the offline RL setting, the replay buffer  $\mathcal{B}$  is replaced by the static dataset  $\mathcal{D}$ . If an OOD action  $a' = \arg \max_{a'} Q(s', a')$  is chosen but is absent from the dataset  $\mathcal{D}$ , the estimated value  $Q(s', a')$  becomes arbitrary and unreliable. Such pathological estimates can destabilize the bootstrapping process.

### 3.2. Support Constraint Policy Improvement

The policy optimization objective of wBC methods are summarized in (Mao et al., 2023), shown as follows,

$$J_\pi^{\text{wBC}}(\phi) = \max_{\phi} \mathbb{E}_{\substack{s \sim \mathcal{D} \\ a \sim \pi_{\text{base}}}} [f(s, a; \pi_{\text{pe}}) \log \pi_\phi(a|s)]. \quad (3)$$

where  $f(s, a; \pi_{\text{pe}}) = \frac{1}{Z(s)} \exp\left(\frac{A^{\pi_{\text{pe}}}(s, a)}{\lambda}\right)$ ,  $Z(s) = \int_a \pi_{\text{base}}(a|s) \exp\left(\frac{A^{\pi_{\text{pe}}}(s, a)}{\lambda}\right) da$  but  $Z(s)$  is usually omitted during training, because errors in the estimation of  $Z(s)$  caused more harm than the benefit the method derived from estimating this value, thereby  $f(s, a; \pi_{\text{pe}}) = \exp\left(\frac{A^{\pi_{\text{pe}}}(s, a)}{\lambda}\right)$ , and  $\lambda$  is a temperature parameter.

Since  $f(s, a; \pi_{\text{pe}}) > 0$ , the policy update of wPC is an equal-support update. Based on the key observation above, STR proposed a support constraint policy improvement method and adopted the Importance Sampling (IS) technique. The objective of policy improvement in STR is designed as follows,

$$J_\pi^{\text{STR}}(\phi) = \max_{\phi} \mathbb{E}_{(s, a) \sim \mathcal{D}} \left[ \frac{\bar{\pi}_\phi(a|s)}{\pi_\beta(a|s)} f(s, a; \bar{\pi}_\phi) \log \pi_\phi(a|s) \right]. \quad (4)$$

where  $\pi_\beta(a|s)$  is behavior policy, and  $\bar{\pi}_\phi(a|s)$  is learned policy but detach of gradient.

### 3.3. IQL

IQL utilizes expectile regression to modify the policy evaluation objective in Eq. (2). The maximum operator is replaced by an upper expectile. In addition, to mitigate the stochasticity introduced by environment dynamics  $s' \sim p(\cdot|s, a)$ , IQL employs a separate value function that estimates an expectile solely with respect to the action distribution. Hence, the update of value function and the  $Q$ -function in IQL during policy evaluation are illustrated below:

$$L_V^{\text{IQL}}(\psi) = \mathbb{E}_{(s, a) \sim \mathcal{D}} [L_2^\tau(Q_{\hat{\theta}}(s, a) - V_\psi(s))]. \quad (5)$$

$$L_Q^{\text{IQL}}(\theta) = \mathbb{E}_{(s, a, s') \sim \mathcal{D}} [(r(s, a) + \gamma V_\psi(s') - Q_\theta(s, a))^2]. \quad (6)$$

where  $L_2^\tau(u) = |\tau - \mathbb{I}(u < 0)|u^2$ , the  $\tau$  expectile of some random variable is defined as a solution to the asymmetric least squares problem, and  $\tau \in (0, 1)$ .

IQL extract the policy using the wBC method. Therefore, the objective of policy improvement in IQL is defined as follows,

$$J_\pi^{\text{IQL}}(\phi) = \max_{\phi} \mathbb{E}_{(s, a) \sim \mathcal{D}} [f(s, a; \pi_\beta) \log \pi_\phi(a|s)]. \quad (7)$$

## 4. Projection IQL with Support Constraint

### 4.1. Policy Evaluation in Proj-IQL

For the sake of simplicity, we define  $\mathbb{E}_{x \sim X}^\tau[x]$  be a  $\tau^{\text{th}}$  expectile of  $X$ , e.g.  $\mathbb{E}^{0.5}$  is the standard expectation. Then the recursive relationship between  $V_\tau(s)$  and  $Q_\tau(s, a)$  are shown as follows,

$$V_\tau(s) = \mathbb{E}_a^\tau [Q_\tau(s, a)]. \quad (8)$$

$$Q_\tau(s, a) = r(s, a) + \gamma \mathbb{E}_{s' \sim p(\cdot|s, a)} [V_\tau(s')]. \quad (9)$$

**Lemma 4.1.** For all  $s$ ,  $\tau_1$  and  $\tau_2$  such that  $\tau_1 < \tau_2$  we get

$$V_{\tau_1}(s) \leq V_{\tau_2}(s).$$

Based on the Lemma. 4.1, a larger  $\tau$  results in a more optimistic policy evaluation, with the  $Q$ -function update approaching the maximum operator in Q-Learning as  $\tau \rightarrow 1$ . Conversely, a smaller  $\tau$  produces a more conservative policy evaluation.

To demonstrate the importance of parameter  $\tau$ , we evaluate the performance of IQL in  $\tau = 0.3, 0.6, 0.9$  on totally 10 D4RL tasks, including 6 Gym-MuJoCo-v2 datasets and 4 AntMaze-v0 datasets. The results, shown in Fig. 1, reveal

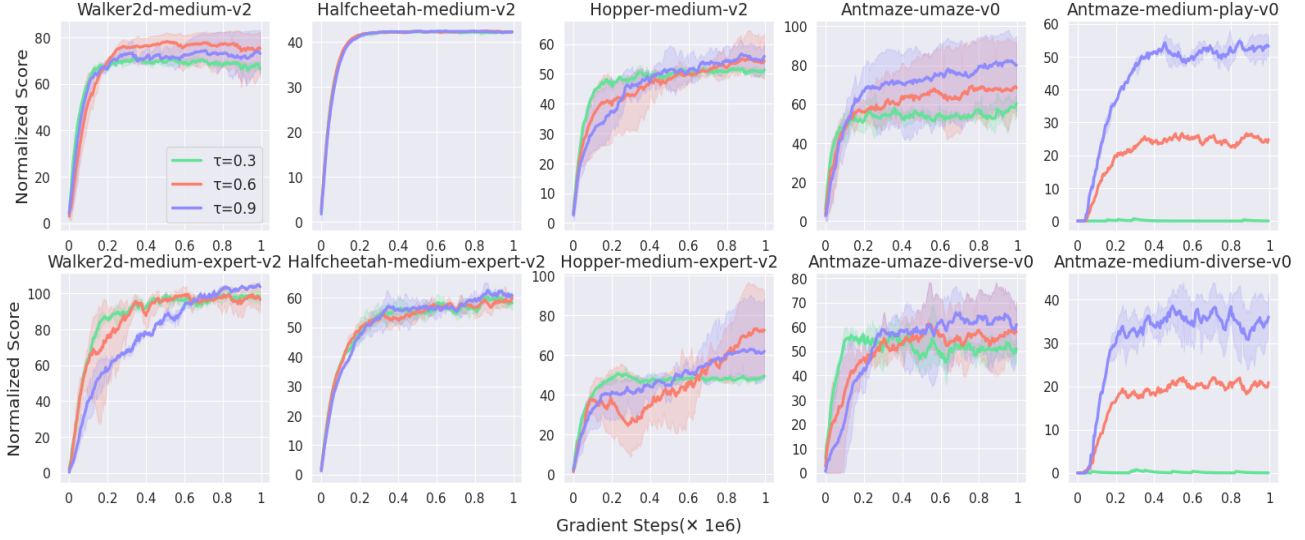


Figure 1. The performance of IQL in  $\tau = 0.3, 0.6, 0.9$  on 10 D4RL datasets, including Walker2d- Halfcheetah- Hopper- medium-v2 and medium-expert-v2 and AntMaze-umaze-v0, AntMaze-umaze-diverse-v0, AntMaze-medium-play-v0, AntMaze-medium-diverse-v0.

that the performance of IQL varies significantly with different values of  $\tau$  on the same dataset, especially in AntMaze-v0 tasks. Therefore, arbitrarily selecting  $\tau$  may not yield optimal results.

Nevertheless, what factors should be considered to determine  $\tau$ ? To address this question, we recap the wBC policy improvement method used in IQL, shown in Eq. (7). Mathematically, this objective function Eq. (7) solves the following two-stage optimization problem,

First stage:

$$\begin{aligned} \pi_{k+1} &= \arg \max_{\pi} \mathbb{E}_{a \sim \pi(\cdot|s)} [A^{\pi_{\beta}}(s, a)], \\ \text{s.t. } &D_{KL}[\pi(\cdot|s) || \pi_{\beta}(\cdot|s)] \leq \epsilon, \\ &\int_a \pi(a|s) da = 1. \end{aligned} \quad (10)$$

Second stage:

$$\pi(\phi) = \arg \min_{\phi} \mathbb{E}_{\rho_{\pi_{\beta}}(s)} [D_{KL}[\pi_{k+1}(\cdot|s) || \pi_{\phi}(\cdot|s)]] . \quad (11)$$

where  $\pi_{k+1}$  denotes the analytical non-parametric solution,  $\pi_{\phi}$  is the parametric policy to approximate  $\pi_{k+1}$  by minimizing the KL divergence, and  $\rho_{\pi_{\beta}}(s)$  signifies the state distribution in the dataset.

According to the optimization problem (10) and (11), the parameter  $\tau$  should first be chosen to reflect the distance  $\mathcal{D}(\pi_{\phi} || \pi_{\beta})$  between the learned policy  $\pi_{\phi}$  and the behavior policy  $\pi_{\beta}$ . As  $\pi_{\phi}$  approaches  $\pi_{\beta}$ ,  $\tau$  should increase optimistically; conversely,  $\tau$  should decrease conservatively as they diverge.

Vector projection provides a way to identify the component of a vector along the direction of another vector. Specifically, the vector projection of vector  $\vec{u}$  onto  $\vec{v}$  is defined as follows,

$$\text{Proj}_{\vec{v}} \vec{u} = \frac{\vec{u} \cdot \vec{v}}{\|\vec{v}\|^2} \vec{v} = \frac{\vec{u} \cdot \vec{v}}{\|\vec{v}\|} \frac{\vec{v}}{\|\vec{v}\|}.$$

where the  $\|\vec{x}\| = \sqrt{\sum_{i=1}^m x_i^2}$  denotes the  $l_2$ -norm of the vector  $\vec{x} \in \mathbb{R}^m$ .

In practice, the learned policy  $\pi_{\phi}$  is approximated by neural networks and represented by a  $K$ -dimensional diagonal Gaussian distribution, where  $K$  represents the dimension of the action space. Typically, the policy networks are trained and updated using batch samples. Given  $n$  input samples  $[(s_1, a_1), (s_2, a_2), \dots, (s_n, a_n)]$ , the policy network outputs  $\vec{\pi}_{\phi}(a|s) = [\pi_{\phi}(a_1|s_1), \pi_{\phi}(a_2|s_2), \dots, \pi_{\phi}(a_n|s_n)]$ . Similarly, the behavior policy  $\pi_{\beta}$  can also be approximated by a neural network, and output  $\vec{\pi}_{\beta}(a|s) = [\pi_{\beta}(a_1|s_1), \pi_{\beta}(a_2|s_2), \dots, \pi_{\beta}(a_n|s_n)]$ .

Therefore, we propose parameter  $\vec{\tau}_{\text{proj}}(a|s)$  based on the vector projection  $\text{Proj}_{\vec{\pi}_{\phi}} \vec{\pi}_{\beta}$  of behavior policy vector  $\vec{\pi}_{\beta}(a|s)$  onto the learned policy vector  $\vec{\pi}_{\phi}(a|s)$ . For one state-action pair, i.e. each component of the vector  $\vec{\tau}_{\text{proj}}(a|s)$ ,  $\tau_{\text{proj}}(a|s)$  is defined as follows,

$$\tau_{\text{proj}}(a|s) = \frac{\vec{\pi}_{\beta}(a|s) \cdot \vec{\pi}_{\phi}(a|s)}{\|\vec{\pi}_{\phi}(a|s)\|^2} \pi_{\phi}(a|s). \quad (12)$$

Based on the  $\tau_{\text{proj}}(a|s)$ , the value function and  $Q$ -function for policy evaluation in Proj-IQL are optimized according to the following loss functions,

$$L_V(\psi) = \mathbb{E}_{(s,a) \sim \mathcal{D}} [L_2^{\tau_{\text{proj}}}(Q_{\hat{\theta}}(s, a) - V_{\psi}(s))]. \quad (13)$$

$$L_Q(\theta) = \mathbb{E}_{(s,a,s') \sim \mathcal{D}} \left[ (r(s,a) + \gamma V_\psi(s') - Q_\theta(s,a))^2 \right]. \quad (14)$$

The advantages of  $\tau_{\text{proj}}(a|s)$  for policy evaluation can be summarized as follows:

#### Advantage 1. Reflect Distance and Adaptively Adjust.

$\tau_{\text{proj}}(a|s)$  represents the length of the shadow of  $\bar{\pi}_\beta(a|s)$  over  $\bar{\pi}_\phi(a|s)$  at state-action pair  $(s,a)$  point. As  $\bar{\pi}_\phi(a|s)$  gets closer to  $\bar{\pi}_\beta(a|s)$ , the larger the projection, the larger  $\tau_{\text{proj}}(a|s)$ , thus allowing for an optimistic evaluation toward the policy  $\pi_\phi(a|s)$ ; conversely, the small  $\tau_{\text{proj}}(a|s)$  allows for a conservative evaluation. The trend of  $\tau_{\text{proj}}(a|s)$  is consistent with the optimization problem (10) and (11).

Moreover,  $\tau_{\text{proj}}(a|s)$  is calculated based on the batch sample under the current policy, not a pre-set hyperparameter. Hence,  $\tau_{\text{proj}}(a|s)$  can also adaptively adjust without the requirement for time-consuming fine-tuning.

#### Advantage 2. Multi-step yet In-sample Learning.

Following the definitions of one-step and multi-step offline RL learning in (Brandfonbrener et al., 2021) and (Mao et al., 2023), when  $f(s,a;\pi_{\text{pe}}) = f(s,a;\pi_\beta)$ , the algorithms are categorized as one-step methods. Based on the objective function in Eq. (7), IQL is classified as a one-step method, which guarantees strict policy improvement only for one step, but without a final performance guarantee.

In contrast, the policy evaluation  $f(s,a;\pi_{\text{pe}}) = f(s,a;\pi_\phi)$  in Proj-IQL can be characterized as a multi-step method while preserving the in-sample learning paradigm. Furthermore, under reasonable assumptions, we demonstrate that the policy evaluation adheres to the expectile regression framework, shown in Theorem 4.2.

**Theorem 4.2.** *If the  $\epsilon$  in the constraint Eq. (10) is sufficiently small <sup>1</sup> for all  $a \in \{\pi_\beta(a|s) > 0, \pi_\phi(a|s) > 0, \text{ and } Q_{\hat{\theta}}(s,a) - V_\psi(s) < 0, \text{ for all } s.\}$ , then Eq. (13) will be transformed as follows,*

$$L_V(\psi) = \mathbb{E}_{\substack{s \sim \mathcal{D}, \\ a \sim \pi_\phi(\cdot|s)}} \left[ L_2^{\bar{\tau}_{\text{proj}}} (Q_{\hat{\theta}}(s,a) - V_\psi(s)) \right].$$

where  $\bar{\tau}_{\text{proj}}(a|s) = \frac{\bar{\pi}_\beta(a|s) \cdot \bar{\pi}_\phi(a|s)}{\|\bar{\pi}_\phi(a|s)\|^2} \pi_\beta(a|s)$ .

Theorem 4.2 states that in Proj-IQL, the policy improvement weight is transformed to  $f(s,a;\pi_\phi)$ , thereby Proj-IQL is a multi-step offline RL algorithm. Meanwhile, Eq. (13) demonstrates that all samples are drawn directly from the dataset, meaning that Proj-IQL belongs to the in-sample learning paradigm. Furthermore, the multi-step Proj-IQL continues to satisfy the expectile regression framework, only change  $\tau_{\text{proj}}(a|s)$  to  $\bar{\tau}_{\text{proj}}(a|s)$ .

<sup>1</sup>Typically,  $\epsilon$  is set small to mitigate the distribution shift resulting from a large discrepancy between  $\pi_\phi$  and  $\pi_\beta$ .

## 4.2. Policy Improvement in Proj-IQL

The policy improvement in IQL is the wBC method, shown in Eq. (7). Nevertheless, directly applying the wBC approach to Proj-IQL does not yield satisfactory results. This is because the policy struggles to converge to the optimal solution when  $\epsilon$  is sufficiently small. Further details and theoretical justification are illuminated in the Lemma 4.3.

**Lemma 4.3.** *If  $D_{KL}[\pi_\phi(\cdot|s) \|\pi_\beta(\cdot|s)] \leq \epsilon, \forall s$  is guaranteed, then the performance  $\eta(\pi) = \mathbb{E}_{\tau \sim \pi} [\sum_{t=0}^{\infty} \gamma^t r_t]$  has the following bound*

$$\eta(\pi_\phi) \leq \eta(\pi_\beta) + \frac{V_{\max}}{\sqrt{2}(1-\gamma)} \sqrt{\epsilon}.$$

where  $0 \leq Q^\pi, V^\pi \leq \frac{R_{\max}}{1-\gamma} =: V_{\max}$ .

Based on the Lemma 4.3, to achieve the optimal policy with high probability,  $\epsilon$  must be set to a large value. However, this requirement contradicts the assumptions of the policy evaluation method, rendering the wBC policy improvement approach unsuitable for Proj-IQL. By contrast, the support constraint-based policy improvement method, as presented in Eq. (4), relaxes the density constraint. Consequently, we adopt the support constraint-based method for policy improvement, shown as follows,

$$J_\pi(\phi) = \max_{\phi} \mathbb{E}_{(s,a) \sim \mathcal{D}} \left[ \frac{\bar{\pi}_\phi(a|s)}{\pi_\beta(a|s)} f(s,a;\bar{\pi}_\phi, \tau_{\text{proj}}) \log \pi_\phi(a|s) \right]. \quad (15)$$

where  $f(s,a;\bar{\pi}_\phi, \tau_{\text{proj}}) = \exp\left(\frac{A_{\tau_{\text{proj}}}^{\bar{\pi}_\phi}(s,a)}{\lambda}\right)$ ,  $A_{\tau_{\text{proj}}}^{\bar{\pi}_\phi}(s,a) = Q_{\tau_{\text{proj}}}^{\bar{\pi}_\phi}(s,a) - V_{\tau_{\text{proj}}}^{\bar{\pi}_\phi}(s)$ .

With an exact tabular  $Q$ -function, we demonstrate that Proj-IQL guarantees strict policy improvement.

**Theorem 4.4.** *If we have exact  $Q$ -function and  $\tau_{k+1}(a|s) \geq \tau_k(a|s)$  <sup>2</sup>, then  $\pi_k$  in Proj-IQL enjoys monotonic improvement:*

$$Q_{\tau_{k+1}}^{\pi_{k+1}}(s,a) \geq Q_{\tau_k}^{\pi_k}(s,a), \quad \forall s,a.$$

Theorem 4.4 establishes that Proj-IQL ensures monotonic policy improvement when policy optimization is performed under support constraint. Compared to the STR algorithm, Proj-IQL shows a significant advantage through its rigorous policy evaluation criterion, which enforces the policy to ‘‘concentrate’’ more effectively on superior actions, where superior actions are defined as  $\{a|Q(s,a) - V(s) \geq 0\}$ .

To illustrate this advantage, we utilize the Monte Carlo estimates approach. Specifically, we sample a large number of

<sup>2</sup>To simplify notation and without ambiguity, we denote the  $\tau_{\text{proj}}(a|s)$  at the  $k$ -th iteration as  $\tau_k(a|s)$ .

actions  $a \sim \pi(\cdot|s)$  and compare the probabilities associated with superior actions. If

$$P \left\{ Q_{\tau_{k+1}}^{\pi_{k+1}}(s, a) - V_{\tau_{k+1}}^{\pi_{k+1}}(s) \geq 0 \right\} \leq P \left\{ Q_{\tau_k}^{\pi_k}(s, a) - V_{\tau_k}^{\pi_k}(s) \geq 0 \right\}. \quad (16)$$

Eq. (16) holds, then we define the evaluation criterion for superior actions as being more rigorous at  $k + 1$ -th iteration, where  $P \{ \mathcal{A} \}$  denotes the probability of event  $\mathcal{A}$ .

We demonstrate that the expectation form of more rigorous evaluation criterion holds when  $a \sim \pi_{k+1}(\cdot|s)$  in Theorem. 4.5.

**Theorem 4.5.** (*Expectation Rigorous Criterion for Superior Actions*). For  $\forall s \in \mathcal{D}$  and  $a \sim \pi_{k+1}(\cdot|s)$ , if  $0.5 \leq \tau_k(a|s), \tau_{k+1}(a|s) \leq 1$ , we have

$$\mathbb{E}_{a \sim \pi_{k+1}(\cdot|s)} \left[ Q_{\tau_{k+1}}^{\pi_{k+1}}(s, a) - V_{\tau_{k+1}}^{\pi_{k+1}}(s) \right] \leq \mathbb{E}_{a \sim \pi_k(\cdot|s)} \left[ Q_{\tau_k}^{\pi_k}(s, a) - V_{\tau_k}^{\pi_k}(s) \right].$$

Theorem. 4.5 illustrates that the expectation of advantage function  $A_{\tau_{k+1}}^{\pi_{k+1}}(s, a)$  under the  $k + 1$ -th iteration policy is lower than the expectation of  $A_{\tau_k}^{\pi_k}(s, a)$ . This result explains the fact that the new policy evaluation criterion for superior actions  $A_{\tau_{k+1}}^{\pi_{k+1}}(s, a)$  is more rigorous than the old one to some extent, as shown in Eq. (16).

Furthermore, Theorem. 4.7 extends result in Theorem. 4.5 to the maximum case of more rigorous evaluation criterion for two arbitrary policies.

**Lemma 4.6.** For any random variable  $X$ , if  $0.5 \leq \tau_1 \leq \tau_2 \leq 1$ , we get

$$\text{Var}^{\tau_1}(X) \leq \text{Var}^{\tau_2}(X).$$

where  $\text{Var}^\tau(X) = \mathbb{E}[(X - \mathbb{E}^\tau(X))^2]$ .

**Theorem 4.7.** (*Maximum Rigorous Criterion for Superior Actions*). For  $\forall s \in \mathcal{D}$ , if  $0.5 \leq \tau_k(a|s) \leq \tau_{k+1}(a|s) \leq 1$ , we have

$$\max_{a \sim \pi_1(\cdot|s)} P \left\{ Q_{\tau_{k+1}}^{\pi_{k+1}}(s, a) - V_{\tau_{k+1}}^{\pi_{k+1}}(s) \geq 0 \right\} \leq \max_{a \sim \pi_2(\cdot|s)} P \left\{ Q_{\tau_k}^{\pi_k}(s, a) - V_{\tau_k}^{\pi_k}(s) \geq 0 \right\}.$$

where  $\pi_1(\cdot|s)$  and  $\pi_2(\cdot|s)$  are arbitrary policies.

### 4.3. Practical Implementation of Proj-IQL

**Behavior Policy** The behavior policy  $\pi_\beta(a|s)$  is approximated using a neural network trained via BC method, as defined in Eq. (17),

$$\pi_\beta(a|s) = \underset{\pi}{\operatorname{argmax}} \mathbb{E}_{(s,a) \sim \mathcal{D}} [\log \pi(a|s)] \quad (17)$$

**Parameter Processing** In both Theorem. 4.5 and Theorem. 4.7, we assume that the projection parameter satisfies  $0.5 \leq \tau_{\text{proj}}(a|s) \leq 1$ . In practice, we enforce this constraint using the *clip* function, defined as follows:

$$\tau_{\text{proj}}(a|s) = \text{clip}(\tau_{\text{proj}}(a|s), 0.5, 1).$$

where  $\text{clip}(x, l, u) = \min(\max(x, l), u)$ .

In practical implementation, we observed that computing  $\tau_{\text{proj}}(a|s)$  for each state-action pair resulted in an overly fine-grained result, which adversely impacted the stability of policy evaluation. To address this issue, we calculate the mean value of  $\tau_{\text{proj}}(a|s)$  across the batch samples, thereby promoting greater stability in the learning process.

**Importance Sampling** To mitigate high variance as well as training instability, we employ the Self-Normalized Importance Sampling (SNIS) method (Mao et al., 2023), which normalizes the IS ratios across the batch.

**Overall Architecture** Integrating the policy evaluation, policy improvement, and practical implementation details, the complete Proj-IQL algorithm is summarized in Algorithm 1.

---

#### Algorithm 1 Proj-IQL

---

**Input:** Dataset  $\mathcal{D} = \{(s, a, s', r)\}$ .

**Initialize Parameters:**  $Q$ -network  $\theta$ , target  $Q$ -network  $\hat{\theta}$ , value network  $\psi$ , policy network  $\phi$ , behavior policy network  $\omega$ .

**for** Behavior Cloning **do**

Optimize behavior policy network  $\omega$  by Eq. (17).

**end for**

**for** Policy Evaluation and Improvement **do**

Random Batch Sample  $(s, a, s', r) \sim \mathcal{D}$ .

Compute  $\tau_{\text{proj}}(a|s)$  by Eq. (12) and mean  $[\tau_{\text{proj}}(a|s)]$ .

Optimize value network  $\psi$  by Eq. (13).

Optimize  $Q$ -network  $\theta$  by Eq. (14).

Optimize policy network  $\phi$  by Eq. (15).

Soft-update target  $Q$ -network  $\theta' \leftarrow (1 - \tau)\theta' + \tau\theta$ .

**end for**

---

## 5. Experiments

In this section, we first evaluate the performance of Proj-IQL on D4RL benchmarks. Additionally, we show the trend of  $\tau_{\text{proj}}(a|s)$  to experimentally confirm the reasonableness of assumption  $\tau_k(a|s) \leq \tau_{k+1}(a|s)$  in Theorem. 4.4 and Theorem. 4.7. Finally, we conduct ablation experiments for different numbers of batch samples.

### 5.1. Comparisons on D4RL Benchmarks

**Gym-MuJoCo Locomotion Tasks** include hopper, halfcheetah, and walker2d environments, which are popular benchmarks used in prior offline RL works. Hence, we

Table 1. Averaged normalized scores on Gym-MuJoCo-v2 datasets. We indicate in bold that the scores are the top-2.

Dataset	DT	RvS	POR	CQL	LAPO	TD3+BC	Reinformer	CRR	IQL	Proj-IQL
halfcheetah-med	42.6	41.6	<b>48.8</b>	44.4	46.0	42.8	42.9	47.1	47.4	<b>48.7±0.45</b>
hopper-med	67.6	60.2	78.6	<b>86.6</b>	51.6	<b>99.5</b>	81.6	38.1	66.3	68.2±13.90
walker2d-med	74.0	71.7	<b>81.1</b>	74.5	80.8	79.7	80.5	59.7	78.3	<b>83.4±0.63</b>
halfcheetah-med-rep	36.6	38.0	43.5	<b>46.2</b>	43.9	43.3	39.0	44.4	44.2	<b>45.5±0.84</b>
hopper-med-rep	82.7	73.5	<b>98.9</b>	48.6	37.6	31.4	83.3	25.5	94.7	<b>95.7±10.63</b>
walker2d-med-rep	66.6	60.6	<b>76.6</b>	32.6	52.3	25.2	72.8	27.0	73.9	<b>89.5±2.68</b>
halfcheetah-med-exp	86.8	92.2	<b>94.7</b>	62.4	86.1	<b>97.9</b>	92.0	85.2	86.7	94.2±1.04
hopper-med-exp	107.6	101.7	90.0	<b>111.0</b>	100.7	<b>112.2</b>	107.8	53.0	91.5	101.5±19.82
walker2d-med-exp	108.1	106.0	109.1	98.7	109.4	101.1	109.3	91.3	<b>109.6</b>	<b>112.2±0.93</b>
Gym-MuJoCo-v2 total	672.6	645.5	<b>721.3</b>	605.0	608.4	633.1	709.2	471.3	692.4	<b>738.9±50.92</b>

compare Proj-IQL against other competitive and widely used baselines such as Decision Transformer (DT) (Chen et al., 2021), RvS (Emmons et al., 2021), POR (Xu et al., 2022), CQL (Kumar et al., 2020), LAPO (Chen et al., 2022), TD3+BC (Fujimoto & Gu, 2021), Reinformer (Zhuang et al., 2024), CRR (Wang et al., 2020) and IQL (Kostrikov et al., 2021). The results are shown in Tab. 1, where we average the mean return over 10 evaluation trajectories and 5 random seeds and calculate the standard deviation.

Despite the performance of different offline RL algorithms on Gym-MuJoCo-v2 datasets being saturated, Proj-IQL still demonstrates strong performance, achieving top-2 rankings on 6 out of 9 tasks and securing the highest overall score across all 9 datasets.

**AntMaze and Kitchen Navigation Tasks** present significantly greater challenges, compared to the Gym-MuJoCo locomotion tasks. The main challenge is to learn policies for long-horizon planning from datasets that do not contain optimal trajectories. Consequently, algorithms must demonstrate strong “stitching” capabilities, combining suboptimal trajectory segments into coherent, high-performing trajectories. We evaluate Proj-IQL against several competitive methods, including Behavior Cloning (BC), BCQ (Fujimoto et al., 2019), BEAR (Kumar et al., 2019), CQL (Kumar et al., 2020), Onestep (Brandfonbrener et al., 2021), TD3+BC (Fujimoto & Gu, 2021), Diffusion-QL (Wang et al., 2022),  $\mathcal{X}$ -QL (Garg et al., 2023), and IQL (Kostrikov et al., 2021), utilizing the same dataset versions as employed in IQL for a fair comparison. The results are presented in Tab. 2.

The Tab. 2 reveal that imitation learning methods such as BC and BCQ struggle to achieve satisfactory results. This limitation arises due to sparse rewards and a large amount of suboptimal trajectories, which place higher demands on algorithms for stable and robust  $Q$ -function and value function estimation. Proj-IQL addresses these challenges by dynamically and adaptively tuning the  $\tau_{proj}$  parameter to estimate the  $Q$ -function and value function according to the current policy. As a result, Proj-IQL demonstrates exceptional performance on the AntMaze-v0 and Kitchen-

v0 datasets, particularly excelling in AntMaze, where it achieves the highest scores on 5 out of the 6 datasets.

### 5.2. The Training Curves of $\tau_{proj}$

In contrast to the fixed hyperparameter  $\tau$  in IQL,  $\tau_{proj}(a|s)$  can be flexibly and adaptively tuned to the current policy and batch samples. Therefore, we plot the  $\tau_{proj}(a|s)$  curve and normalized score curve on AntMaze-v0 and Kitchen-v0 datasets. The results are shown in Fig. 2.

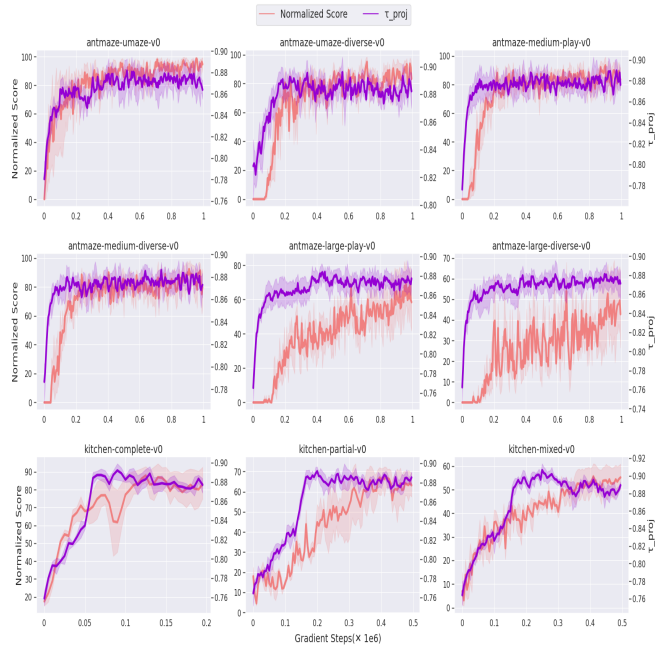


Figure 2. The training curves of normalized score and  $\tau_{proj}(a|s)$  on AntMaze-v0 and Kitchen-v0 datasets. The solid line and shaded regions represent the mean and standard deviation, respectively.

Based on Fig. 2, we observed that the curve  $\tau_{proj}(a|s)$  exhibits an upward trend, reflecting an increase in the projected component of  $\pi_\phi(a|s)$  within  $\pi_\beta(a|s)$ . This phenomenon arises because, in Proj-IQL, the updated method of policy can be seen as a weighted behavior cloning as

Table 2. Averaged normalized scores on AntMaze-v0 and Kitchen-v0 datasets. We indicate in bold that the scores are the top-2.

Dataset	BC	BCQ	BEAR	CQL	Onestep	TD3+BC	Diffusion-QL	$\lambda$ -QL	IQL	Proj-IQL
antmaze-umaze	54.6	78.9	73.0	74.0	62.4	78.6	93.4	<b>93.8</b>	87.5	<b>98.0±6.0</b>
antmaze-umaze-diverse	45.6	55.0	61.0	<b>84.0</b>	44.7	71.4	66.2	82.0	62.2	<b>98.0±6.0</b>
antmaze-med-play	0.0	0.0	0.0	61.2	5.4	10.6	<b>76.6</b>	76.0	71.2	<b>94.0±14.0</b>
antmaze-med-diverse	0.0	0.0	8.0	53.7	1.8	3.0	<b>78.6</b>	73.6	70.0	<b>88.0±8.0</b>
antmaze-large-play	0.0	6.7	0.0	15.8	0.1	0.2	46.4	<b>46.5</b>	39.6	<b>72.0±9.8</b>
antmaze-large-diverse	0.0	2.2	0.0	14.9	0.9	0.0	<b>56.6</b>	49.0	47.5	<b>50.0±10.0</b>
AntMaze-v0 total	100.2	142.8	142.0	303.6	115.2	163.8	417.8	<b>420.9</b>	378.0	<b>500.0±53.8</b>
kitchen-complete	65.0	8.1	0.0	43.8	66.0	61.5	<b>84.0</b>	82.4	62.5	<b>87.0±4.6</b>
kitchen-partial	38.0	18.9	13.1	49.8	59.3	52.8	60.5	<b>73.7</b>	46.3	<b>67.0±6.0</b>
kitchen-mixed	51.5	8.1	47.2	51.0	56.5	60.8	<b>62.6</b>	<b>62.5</b>	51.0	55.5±3.2
Kitchen-v0 total	154.5	35.1	60.3	144.6	181.7	175.1	207.1	<b>218.6</b>	159.8	<b>209.5±13.8</b>

described in Eq.(15), where the weight factor is given by  $\frac{\bar{\pi}_\phi(a|s)}{\pi_\beta(a|s)} \exp\left(\frac{A_{\tau_{proj}}(s,a)}{\lambda}\right) > 0$ . However, this weight is essentially different with the weight in the aforementioned wBC method. Furthermore, this upward trend supports our assumption  $0.5 \leq \tau_k(a|s) \leq \tau_{k+1}(a|s) \leq 1$  as stated in Theorem. 4.4 and Theorem. 4.7.

Another noteworthy observation is that the rise in normalized scores lags behind the  $\tau_{proj}(a|s)$  parameter, indicating that updates to  $\tau_{proj}(a|s)$  contribute to more accurate estimates of the  $Q$ -function and value function. Then, the more accurate estimates facilitate continuous policy improvement, resulting in higher normalized scores. However, this phenomenon is less apparent in the kitchen-complete-v0 dataset, since this dataset is relatively small with only 3, 680 samples. In contrast, datasets such as AntMaze-v0 typically contain approximately  $10^6$  samples, and other Kitchen-v0 datasets include 136, 950 samples.

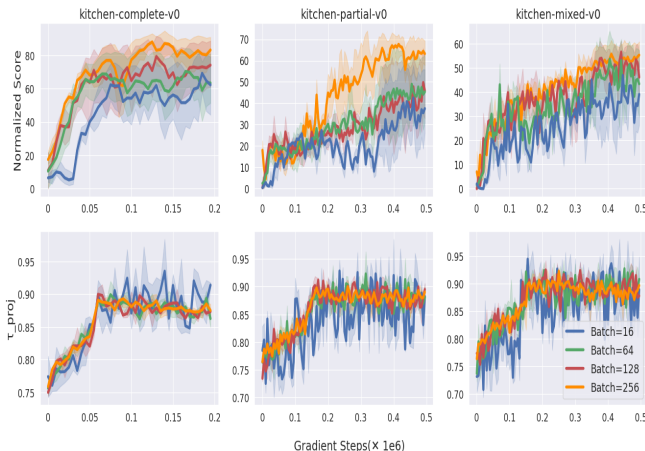


Figure 3. The training curves of normalized score and  $\tau_{proj}(a|s)$  on Kitchen-v0 datasets under  $batch\ size = 16, 64, 128, 256$ . The solid line and shaded regions represent the mean and standard deviation, respectively.

### 5.3. Empirical Study on the Projection Parameter

In the proposed Proj-IQL method, each sample in the batch is treated as a component of the vector used to compute  $\tau_{proj}(a|s)$ , making the *batch size* to be one of the critical parameters. To investigate this, we evaluated the performance of  $\tau_{proj}(a|s)$  as well as normalized scores corresponding  $batch\ size = 16, 64, 128, 256$  on three Kitchen-v0 datasets. The results are presented in Fig. 3.

As shown in Fig. 3, the normalized score gradually increases with larger batch sizes, which aligns with expectations. This improvement occurs because larger batch sizes allow both the policy and value networks to be trained more effectively. However, this trend does not fully capture the specific impact of batch size on the parameter  $\tau_{proj}(a|s)$ . To address this issue, we also plotted the relationship between batch size and  $\tau_{proj}(a|s)$ . The results clearly indicate that the stability of  $\tau_{proj}(a|s)$  improves as the batch size increases, with reduced fluctuations. A more stable  $\tau_{proj}(a|s)$  is particularly beneficial for enhancing performance because of the policy evaluation is more stable.

## 6. Conclusion

We propose Proj-IQL, an in-sample, multi-step, support-constrained offline RL algorithm based on IQL. During the policy evaluation phase, Proj-IQL transitions from a one-step approach to a multi-step in-sample offline RL algorithm while preserving the expectile regression framework. In the policy improvement phase, Proj-IQL incorporates a support constraint to facilitate effective policy updates. Furthermore, we provide a theoretical foundation, demonstrating the invariance of the expectile regression framework, monotonic policy improvement guarantees, and a more rigorous policy evaluation criterion. Empirical results validate the theoretical insights of Proj-IQL and highlight its state-of-the-art performance on D4RL benchmarks, particularly excelling in challenging AntMaze-v0 and Kitchen-0 navigation tasks. In the future, Proj-IQL will be improved to more efficient learning policies on less amount of data.

## References

- Brandfonbrener, D., Whitney, W., Ranganath, R., and Bruna, J. Offline rl without off-policy evaluation. *Advances in neural information processing systems*, 34:4933–4946, 2021.
- Chen, L., Lu, K., Rajeswaran, A., Lee, K., Grover, A., Laskin, M., Abbeel, P., Srinivas, A., and Mordatch, I. Decision transformer: Reinforcement learning via sequence modeling. *Advances in neural information processing systems*, 34:15084–15097, 2021.
- Chen, L., Yan, J., Shao, Z., Wang, L., Lin, Q., Rajmohan, S., Moscibroda, T., and Zhang, D. Conservative state value estimation for offline reinforcement learning. *Advances in Neural Information Processing Systems*, 36, 2024.
- Chen, X., Ghadirzadeh, A., Yu, T., Wang, J., Gao, A. Y., Li, W., Bin, L., Finn, C., and Zhang, C. Lapo: Latent-variable advantage-weighted policy optimization for offline reinforcement learning. *Advances in Neural Information Processing Systems*, 35:36902–36913, 2022.
- Emmons, S., Eysenbach, B., Kostrikov, I., and Levine, S. Rvs: What is essential for offline rl via supervised learning? *arXiv preprint arXiv:2112.10751*, 2021.
- Fu, J., Kumar, A., Nachum, O., Tucker, G., and Levine, S. D4rl: Datasets for deep data-driven reinforcement learning. *arXiv preprint arXiv:2004.07219*, 2020.
- Fujimoto, S. and Gu, S. S. A minimalist approach to offline reinforcement learning. *Advances in neural information processing systems*, 34:20132–20145, 2021.
- Fujimoto, S., Meger, D., and Precup, D. Off-policy deep reinforcement learning without exploration. In *International conference on machine learning*, pp. 2052–2062. PMLR, 2019.
- Garg, D., Hejna, J., Geist, M., and Ermon, S. Extreme q-learning: Maxent rl without entropy. *arXiv preprint arXiv:2301.02328*, 2023.
- Han, X., Afifi, H., Moun gla, H., and Marot, M. Leaky ppo: A simple and efficient rl algorithm for autonomous vehicles. In *2024 International Joint Conference on Neural Networks (IJCNN)*, pp. 1–7. IEEE, 2024.
- Kostrikov, I., Nair, A., and Levine, S. Offline reinforcement learning with implicit q-learning. *arXiv preprint arXiv:2110.06169*, 2021.
- Kumar, A., Fu, J., Soh, M., Tucker, G., and Levine, S. Stabilizing off-policy q-learning via bootstrapping error reduction. *Advances in neural information processing systems*, 32, 2019.
- Kumar, A., Zhou, A., Tucker, G., and Levine, S. Conservative q-learning for offline reinforcement learning. *Advances in Neural Information Processing Systems*, 33: 1179–1191, 2020.
- Levine, S., Kumar, A., Tucker, G., and Fu, J. Offline reinforcement learning: Tutorial, review, and perspectives on open problems. *arXiv preprint arXiv:2005.01643*, 2020.
- Mao, Y., Zhang, H., Chen, C., Xu, Y., and Ji, X. Supported trust region optimization for offline reinforcement learning. In *International Conference on Machine Learning*, pp. 23829–23851. PMLR, 2023.
- Mao, Y., Zhang, H., Chen, C., Xu, Y., and Ji, X. Supported value regularization for offline reinforcement learning. *Advances in Neural Information Processing Systems*, 36, 2024.
- Nair, A., Gupta, A., Dalal, M., and Levine, S. Awac: Accelerating online reinforcement learning with offline datasets. *arXiv preprint arXiv:2006.09359*, 2020.
- Peng, X. B., Kumar, A., Zhang, G., and Levine, S. Advantage-weighted regression: Simple and scalable off-policy reinforcement learning. *arXiv preprint arXiv:1910.00177*, 2019.
- Peng, Z., Liu, Y., Chen, H., and Zhou, Z. Conservative network for offline reinforcement learning. *Knowledge-Based Systems*, 282:111101, 2023.
- Peters, J. and Schaal, S. Reinforcement learning by reward-weighted regression for operational space control. In *Proceedings of the 24th international conference on machine learning*, pp. 745–750, 2007.
- Pomerleau, D. A. Efficient training of artificial neural networks for autonomous navigation. *Neural computation*, 3(1):88–97, 1991.
- Prudencio, R. F., Maximo, M. R., and Colombini, E. L. A survey on offline reinforcement learning: Taxonomy, review, and open problems. *IEEE Transactions on Neural Networks and Learning Systems*, 2023.
- Sutton, R. S. and Barto, A. G. *Reinforcement learning: An introduction*. MIT press, 2018.
- Vuong, Q., Kumar, A., Levine, S., and Chebotar, Y. Dasco: Dual-generator adversarial support constrained offline reinforcement learning. *Advances in Neural Information Processing Systems*, 35:38937–38949, 2022.
- Wang, Z., Novikov, A., Zolna, K., Merel, J. S., Springenberg, J. T., Reed, S. E., Shahriari, B., Siegel, N., Gulcehre, C., Heess, N., et al. Critic regularized regression. *Advances in Neural Information Processing Systems*, 33: 7768–7778, 2020.

- Wang, Z., Hunt, J. J., and Zhou, M. Diffusion policies as an expressive policy class for offline reinforcement learning. *arXiv preprint arXiv:2208.06193*, 2022.
- Wu, J., Wu, H., Qiu, Z., Wang, J., and Long, M. Supported policy optimization for offline reinforcement learning. *Advances in Neural Information Processing Systems*, 35: 31278–31291, 2022.
- Wu, K., Zhao, Y., Xu, Z., Che, Z., Yin, C., Liu, C. H., Qiu, Q., Feng, F., and Tang, J. Acl-ql: Adaptive conservative level in  $q$ -learning for offline reinforcement learning. *IEEE Transactions on Neural Networks and Learning Systems*, 2024.
- Xu, H., Jiang, L., Jianxiong, L., and Zhan, X. A policy-guided imitation approach for offline reinforcement learning. *Advances in Neural Information Processing Systems*, 35:4085–4098, 2022.
- Xu, H., Jiang, L., Li, J., Yang, Z., Wang, Z., Chan, V. W. K., and Zhan, X. Offline rl with no ood actions: In-sample learning via implicit value regularization. *arXiv preprint arXiv:2303.15810*, 2023.
- Zhang, C., Kuppannagari, S., and Viktor, P. Brac+: Improved behavior regularized actor critic for offline reinforcement learning. In *Asian Conference on Machine Learning*, pp. 204–219. PMLR, 2021.
- Zhou, W., Bajracharya, S., and Held, D. Plas: Latent action space for offline reinforcement learning. In *Conference on Robot Learning*, pp. 1719–1735. PMLR, 2021.
- Zhuang, Z., Peng, D., Liu, J., Zhang, Z., and Wang, D. Reinformers: Max-return sequence modeling for offline rl. *arXiv preprint arXiv:2405.08740*, 2024.

## A. Proofs

### Proof of Lemma. 4.1.

Lemma 4.1. For all  $s$ ,  $\tau_1$  and  $\tau_2$  such that  $\tau_1 < \tau_2$  we get

$$V_{\tau_1}(s) \leq V_{\tau_2}(s).$$

*Proof.* The proof follows the Lemma.2 proof in (Kostrikov et al., 2021).  $\square$

### Proof of Theorem. 4.2.

Theorem 4.2. If the  $\epsilon$  in the constraint Eq. (10) is sufficiently small for all  $a \in \{\pi_\beta(a|s) > 0, \pi_\phi(a|s) > 0, \text{ and } Q_{\hat{\theta}}(s, a) - V_\psi(s) < 0, \text{ for all } s.\}$ , then Eq. (13) will be transformed as follows,

$$L_V(\psi) = \mathbb{E}_{\substack{s \sim \mathcal{D}, \\ a \sim \pi_\phi(\cdot|s)}} \left[ L_2^{\bar{\tau}_{proj}}(Q_{\hat{\theta}}(s, a) - V_\psi(s)) \right].$$

where  $\bar{\tau}_{proj}(a|s) = \frac{\bar{\pi}_\beta(a|s) \cdot \bar{\pi}_\phi(a|s)}{\|\bar{\pi}_\phi(a|s)\|^2} \pi_\beta(a|s)$ .

*Proof.* For one state-action pair  $(s, a)$ , the  $\tau_{proj}(a|s)$  is defined as Eq. (12). We bring the  $\tau_{proj}(a|s)$  into Eq. (13) and expand,

$$\begin{aligned} L_V(\psi) &= \mathbb{E}_{(s,a) \sim \mathcal{D}} \left[ L_2^{\tau_{proj}}(Q_{\hat{\theta}}(s, a) - V_\psi(s)) \right] \\ &= \begin{cases} \mathbb{E}_{(s,a) \sim \mathcal{D}} \left[ \tau_{proj}(Q_{\hat{\theta}}(s, a) - V_\psi(s))^2 \right], & \text{if } Q_{\hat{\theta}}(s, a) - V_\psi(s) \geq 0; \\ \mathbb{E}_{(s,a) \sim \mathcal{D}} \left[ (1 - \tau_{proj})(Q_{\hat{\theta}}(s, a) - V_\psi(s))^2 \right], & \text{if } Q_{\hat{\theta}}(s, a) - V_\psi(s) < 0. \end{cases} \end{aligned} \quad (18)$$

①. For  $Q_{\hat{\theta}}(s, a) - V_\psi(s) \geq 0$ ,

$$\begin{aligned} L_V^{Q \geq V}(\psi) &= \mathbb{E}_{(s,a) \sim \mathcal{D}} \left[ \tau_{proj}(Q_{\hat{\theta}}(s, a) - V_\psi(s))^2 \right] \\ &= \mathbb{E}_{\substack{s \sim \mathcal{D}, \\ a \sim \pi_\beta(\cdot|s)}} \left[ \frac{\bar{\pi}_\beta(a|s) \cdot \bar{\pi}_\phi(a|s)}{\|\bar{\pi}_\phi(a|s)\|^2} \pi_\phi(a|s) (Q_{\hat{\theta}}(s, a) - V_\psi(s))^2 \right] \\ &= \mathbb{E}_{\substack{s \sim \mathcal{D}, \\ a \sim \pi_\phi(\cdot|s)}} \left[ \frac{\bar{\pi}_\beta(a|s) \cdot \bar{\pi}_\phi(a|s)}{\|\bar{\pi}_\phi(a|s)\|^2} \pi_\beta(a|s) (Q_{\hat{\theta}}(s, a) - V_\psi(s))^2 \right]. \end{aligned} \quad (19)$$

②. For  $Q_{\hat{\theta}}(s, a) - V_\psi(s) < 0$ ,

$$\begin{aligned} L_V^{Q < V}(\psi) &= \mathbb{E}_{(s,a) \sim \mathcal{D}} \left[ (1 - \tau_{proj})(Q_{\hat{\theta}}(s, a) - V_\psi(s))^2 \right] \\ &= \mathbb{E}_{\substack{s \sim \mathcal{D}, \\ a \sim \pi_\beta(\cdot|s)}} \left[ \left( 1 - \frac{\bar{\pi}_\beta(a|s) \cdot \bar{\pi}_\phi(a|s)}{\|\bar{\pi}_\phi(a|s)\|^2} \pi_\phi(a|s) \right) (Q_{\hat{\theta}}(s, a) - V_\psi(s))^2 \right] \\ &= \mathbb{E}_{\substack{s \sim \mathcal{D}, \\ a \sim \pi_\beta(\cdot|s)}} \left[ (Q_{\hat{\theta}}(s, a) - V_\psi(s))^2 \right] - L_V^{Q \geq V}(\psi). \end{aligned} \quad (20)$$

In addition, we calculate

$$\begin{aligned}
 & \left| \mathbb{E}_{\substack{s \sim \mathcal{D}, \\ a \sim \pi_\phi(\cdot|s)}} [(Q_{\hat{\theta}}(s, a) - V_\psi(s))^2] - \mathbb{E}_{\substack{s \sim \mathcal{D}, \\ a \sim \pi_\beta(\cdot|s)}} [(Q_{\hat{\theta}}(s, a) - V_\psi(s))^2] \right| \\
 &= \left| \mathbb{E}_{s \sim \mathcal{D}} \left[ \int (\pi_\phi(a|s) - \pi_\beta(a|s)) (Q_{\hat{\theta}}(s, a) - V_\psi(s))^2 da \right] \right| \\
 &\leq \mathbb{E}_{s \sim \mathcal{D}} \left[ \int |\pi_\phi(a|s) - \pi_\beta(a|s)| (Q_{\hat{\theta}}(s, a) - V_\psi(s))^2 da \right] \\
 &\leq \mathbb{E}_{s \sim \mathcal{D}} \left[ \int D_{TV}(\pi_\phi(\cdot|s) \| \pi_\beta(\cdot|s)) (Q_{\hat{\theta}}(s, a) - V_\psi(s))^2 da \right] \\
 &\leq \frac{1}{\sqrt{2}} \mathbb{E}_{s \sim \mathcal{D}} \left[ \int \sqrt{D_{KL}(\pi_\phi(\cdot|s) \| \pi_\beta(\cdot|s))} (Q_{\hat{\theta}}(s, a) - V_\psi(s))^2 da \right] \quad (\text{Pinsker's Inequality}) \\
 &\leq \sqrt{\frac{\epsilon}{2}} \mathbb{E}_{s \sim \mathcal{D}} \left[ \int (Q_{\hat{\theta}}(s, a) - V_\psi(s))^2 da \right].
 \end{aligned} \tag{21}$$

Under the assumption that the  $\epsilon$  in the constraint of Eq. (10) is sufficiently small, we have the difference between  $\mathbb{E}_{s \sim \mathcal{D}, a \sim \pi_\phi(\cdot|s)} [(Q_{\hat{\theta}}(s, a) - V_\psi(s))^2]$  and  $\mathbb{E}_{s \sim \mathcal{D}, a \sim \pi_\beta(\cdot|s)} [(Q_{\hat{\theta}}(s, a) - V_\psi(s))^2]$  is enough small based on the Eq. (21).

Therefore, for  $Q_{\hat{\theta}}(s, a) - V_\psi(s) < 0$ , we can rewrite the Eq. (20) as follow,

$$\begin{aligned}
 L_V^{Q < V}(\psi) &= \mathbb{E}_{\substack{s \sim \mathcal{D}, \\ a \sim \pi_\beta(\cdot|s)}} [(Q_{\hat{\theta}}(s, a) - V_\psi(s))^2] - L_V^{Q \geq V}(\psi) \\
 &\approx \mathbb{E}_{\substack{s \sim \mathcal{D}, \\ a \sim \pi_\phi(\cdot|s)}} [(Q_{\hat{\theta}}(s, a) - V_\psi(s))^2] - L_V^{Q \geq V}(\psi) \\
 &= \mathbb{E}_{\substack{s \sim \mathcal{D}, \\ a \sim \pi_\phi(\cdot|s)}} \left[ \left( 1 - \frac{\bar{\pi}_\beta(a|s) \cdot \bar{\pi}_\phi(a|s)}{\|\bar{\pi}_\phi(a|s)\|^2} \pi_\beta(a|s) \right) (Q_{\hat{\theta}}(s, a) - V_\psi(s))^2 \right].
 \end{aligned} \tag{22}$$

Combining Eq. (19) and (22), we obtain

$$L_V(\psi) = \mathbb{E}_{\substack{s \sim \mathcal{D}, \\ a \sim \pi_\phi(\cdot|s)}} \left[ L_2^{\bar{\tau}_{\text{proj}}} (Q_{\hat{\theta}}(s, a) - V_\psi(s)) \right]. \tag{23}$$

where  $\bar{\tau}_{\text{proj}}(a|s) = \frac{\bar{\pi}_\beta(a|s) \cdot \bar{\pi}_\phi(a|s)}{\|\bar{\pi}_\phi(a|s)\|^2} \pi_\beta(a|s)$ . □

### Proof of Lemma. 4.3.

**Lemma 4.3.** *If  $D_{KL}[\pi_\phi(\cdot|s) \| \pi_\beta(\cdot|s)] \leq \epsilon$ ,  $\forall s$  is guaranteed, then the performance  $\eta(\pi) = \mathbb{E}_{\tau \sim \pi} [\sum_{t=0}^{\infty} \gamma^t r_t]$  has the following bound*

$$\eta(\pi_\phi) \leq \eta(\pi_\beta) + \frac{V_{\max}}{\sqrt{2}(1-\gamma)} \sqrt{\epsilon}.$$

where  $0 \leq Q^\pi, V^\pi \leq \frac{R_{\max}}{1-\gamma} =: V_{\max}$ .

*Proof.* The proof follows the Lemma 3.1 proof in (Mao et al., 2023). □

### Proof of Theorem. 4.4.

**Theorem 4.4.** *If we have exact  $Q$ -function and  $\tau_{k+1}(a|s) \geq \tau_k(a|s)$ , then  $\pi_k$  in Proj-IQL enjoys monotonic improvement:*

$$Q_{\tau_{k+1}}^{\pi_{k+1}}(s, a) \geq Q_{\tau_k}^{\pi_k}(s, a), \quad \forall s, a.$$

*Proof.* The  $\pi_\phi(a|s)$  under the policy improvement objective Eq. (15) is a parametric approximation of

$$\pi_{k+1}(a|s) = \frac{1}{Z_k(s)} \pi_k(a|s) \exp\left(\frac{A_{\tau_k}^{\pi_k}(s, a)}{\lambda}\right). \quad (24)$$

where  $Z_k(s) = \int_a \pi_k(a|s) \exp\left(\frac{A_{\tau_k}^{\pi_k}(s, a)}{\lambda}\right) da$ , and  $A_{\tau_k}^{\pi_k}(s, a) = Q_{\tau_k}^{\pi_k}(s, a) - V_{\tau_k}^{\pi_k}(s)$ .

Based on the wBC policy extraction methods, the Eq. (24) is the optimal solution for the following optimization problem,

$$\begin{aligned} \pi_{k+1} &= \arg \max_{\pi \in \Pi} \mathbb{E}_{a \sim \pi(\cdot|s)} [Q_{\tau_k}^{\pi_k}(s, a)], \\ \text{s.t. } &D_{KL}[\pi(\cdot|s) || \pi_k(\cdot|s)] \leq \epsilon, \\ &\int_a \pi(a|s) da = 1. \end{aligned} \quad (25)$$

Because  $D_{KL}[\pi_k(\cdot|s) || \pi_k(\cdot|s)] = 0 < \epsilon$ ,  $\forall s$  is a strictly feasible solution. Therefore,  $\mathbb{E}_{a \sim \pi_{k+1}} [Q_{\tau_k}^{\pi_k}(s, a)] \geq \mathbb{E}_{a \sim \pi_k} [Q_{\tau_k}^{\pi_k}(s, a)]$ ,  $\forall s$ . It implies

$$\begin{aligned} &Q_{\tau_k}^{\pi_k}(s, a) \\ &= r(s, a) + \gamma \mathbb{E}_{s_{t+1} \sim p(\cdot|s_t, a_t)} \mathbb{E}_{a \sim \pi_k} [Q_{\tau_k}^{\pi_k}(s_{t+1}, a_{t+1}) | s_t = s, a_t = a] \\ &\leq r(s, a) + \gamma \mathbb{E}_{s_{t+1} \sim p(\cdot|s_t, a_t)} \mathbb{E}_{a \sim \pi_{k+1}} [Q_{\tau_k}^{\pi_k}(s_{t+1}, a_{t+1}) | s_t = s, a_t = a] \\ &\quad \dots \\ &\leq \mathbb{E}_{a \sim \pi_{k+1}} \left[ \sum_{n=0}^{\infty} \gamma^n r(s_{t+n}, a_{t+n}) | s_t = s, a_t = a \right] \\ &= Q_{\tau_k}^{\pi_{k+1}}(s, a). \end{aligned}$$

Therefore,  $Q_{\tau_k}^{\pi_{k+1}}(s, a) \geq Q_{\tau_k}^{\pi_k}(s, a)$ ,  $\forall s, a$ .

Then, we rewrite  $Q_{\tau_k}^{\pi_{k+1}}(s, a)$  as

$$\begin{aligned} &Q_{\tau_k}^{\pi_{k+1}}(s, a) \\ &= r(s, a) + \gamma \mathbb{E}_{s_{t+1} \sim p(\cdot|s_t, a_t)} [V_{\tau_k}^{\pi_{k+1}}(s_{t+1}) | s_t = s, a_t = a] \\ &\leq r(s, a) + \gamma \mathbb{E}_{s_{t+1} \sim p(\cdot|s_t, a_t)} [V_{\tau_{k+1}}^{\pi_{k+1}}(s_{t+1}) | s_t = s, a_t = a] \quad (\text{Lemma. 4.1}) \\ &= Q_{\tau_{k+1}}^{\pi_{k+1}}(s, a). \end{aligned}$$

Therefore,  $Q_{\tau_{k+1}}^{\pi_{k+1}}(s, a) \geq Q_{\tau_k}^{\pi_{k+1}}(s, a) \geq Q_{\tau_k}^{\pi_k}(s, a)$ ,  $\forall s, a$  □

#### Proof of Theorem. 4.5.

**Theorem 4.5.** (*Expectation Rigorous Criterion for Superior Actions*). For  $\forall s \in \mathcal{D}$  and  $a \sim \pi_{k+1}(\cdot|s)$ , if  $0.5 \leq \tau_k(a|s), \tau_{k+1}(a|s) \leq 1$ , we have

$$\mathbb{E}_{a \sim \pi_{k+1}(\cdot|s)} [Q_{\tau_{k+1}}^{\pi_{k+1}}(s, a) - V_{\tau_{k+1}}^{\pi_{k+1}}(s)] \leq \mathbb{E}_{a \sim \pi_{k+1}(\cdot|s)} [Q_{\tau_k}^{\pi_k}(s, a) - V_{\tau_k}^{\pi_k}(s)].$$

*Proof.* For the left-hand side of the above inequality,

$$\begin{aligned} &\mathbb{E}_{a \sim \pi_{k+1}(\cdot|s)} [Q_{\tau_{k+1}}^{\pi_{k+1}}(s, a) - V_{\tau_{k+1}}^{\pi_{k+1}}(s)] \\ &= \mathbb{E}_{a \sim \pi_{k+1}(\cdot|s)} [Q_{\tau_{k+1}}^{\pi_{k+1}}(s, a)] - V_{\tau_{k+1}}^{\pi_{k+1}}(s) \\ &= V^{\pi_{k+1}}(s) - V_{\tau_{k+1}}^{\pi_{k+1}}(s) \\ &\leq 0. \quad (\text{Lemma. 4.1}) \end{aligned} \quad (26)$$

For the right-hand side of the inequality,

$$\begin{aligned}
 & \mathbb{E}_{a \sim \pi_{k+1}(\cdot|s)} [Q_{\tau_k}^{\pi_k}(s, a) - V_{\tau_k}^{\pi_k}(s)] \\
 &= \mathbb{E}_{a \sim \pi_{k+1}(\cdot|s)} [Q_{\tau_k}^{\pi_k}(s, a)] - V_{\tau_k}^{\pi_k}(s) \\
 &= \mathbb{E}_{a \sim \pi_k(\cdot|s)}^{\tau \rightarrow 1} [Q_{\tau_k}^{\pi_k}(s, a)] - V_{\tau_k}^{\pi_k}(s) \quad (\text{Eq. (25) \& Theorem. 4.4}) \\
 &= V_{\tau \rightarrow 1}^{\pi_k}(s) - V_{\tau_k}^{\pi_k}(s) \\
 &\geq 0. \quad (\text{Lemma. 4.1})
 \end{aligned} \tag{27}$$

Therefore, Theorem. 4.5 holds.  $\square$

### Proof of Lemma. 4.6.

Lemma 4.6. For any random variable  $X$ , if  $0.5 \leq \tau_1 \leq \tau_2 \leq 1$ , we get

$$\text{Var}^{\tau_1}(X) \leq \text{Var}^{\tau_2}(X).$$

where  $\text{Var}^\tau(X) = \mathbb{E}[(X - \mathbb{E}^\tau(X))^2]$ .

*Proof.* We calculate

$$\begin{aligned}
 & \text{Var}^{\tau_1}(X) - \text{Var}^{\tau_2}(X) \\
 &= \mathbb{E}(X^2) - 2\mathbb{E}(X)\mathbb{E}^{\tau_1}(X) + \mathbb{E}^{\tau_1}(X)^2 - \mathbb{E}(X^2) + 2\mathbb{E}(X)\mathbb{E}^{\tau_2}(X) - \mathbb{E}^{\tau_2}(X)^2 \\
 &= \underbrace{[\mathbb{E}^{\tau_1}(X) + \mathbb{E}^{\tau_2}(X) - 2\mathbb{E}(X)]}_{\geq 0} \underbrace{[\mathbb{E}^{\tau_1}(X) - \mathbb{E}^{\tau_2}(X)]}_{\leq 0} \quad (\text{Lemma.4.1 and } 0.5 \leq \tau_1 \leq \tau_2 \leq 1) \\
 &\leq 0.
 \end{aligned}$$

Therefore,  $\text{Var}^{\tau_1}(X) - \text{Var}^{\tau_2}(X) \leq 0$ .  $\square$

### Proof of Theorem. 4.7.

Theorem 4.7. (Maximum Rigorous Criterion for Superior Actions). For  $\forall s \in \mathcal{D}$ , if  $0.5 \leq \tau_k(a|s) \leq \tau_{k+1}(a|s) \leq 1$ , we have

$$\max_{a \sim \pi_1(\cdot|s)} P \left\{ Q_{\tau_{k+1}}^{\pi_{k+1}}(s, a) - V_{\tau_{k+1}}^{\pi_{k+1}}(s) \geq 0 \right\} \leq \max_{a \sim \pi_2(\cdot|s)} P \left\{ Q_{\tau_k}^{\pi_k}(s, a) - V_{\tau_k}^{\pi_k}(s) \geq 0 \right\}.$$

where  $\pi_1(\cdot|s)$  and  $\pi_2(\cdot|s)$  are arbitrary policies.

*Proof.* Firstly, we define

$$\mathbb{E}_{a \sim \pi_{k+1}}^{\tau_{k+1}} [Q_{\tau_{k+1}}^{\pi_{k+1}}(s, a)] - \mathbb{E}_{a \sim \pi_{k+1}} [Q_{\tau_{k+1}}^{\pi_{k+1}}(s, a)] = \epsilon_1. \tag{28}$$

$$\mathbb{E}_{a \sim \pi_k}^{\tau_k} [Q_{\tau_k}^{\pi_k}(s, a)] - \mathbb{E}_{a \sim \pi_k} [Q_{\tau_k}^{\pi_k}(s, a)] = \epsilon_2. \tag{29}$$

Because  $0.5 \leq \tau_k(a|s) \leq \tau_{k+1}(a|s) \leq 1$  and Lemma. 4.1,  $\epsilon_1, \epsilon_2 \geq 0$ .

Next, we found that for any random variable  $X$ ,

$$\begin{aligned}
 & \text{Var}^\tau(X) - \text{Var}(X) \\
 &= \mathbb{E}(X^2) - 2\mathbb{E}(X)\mathbb{E}^\tau(X) + \mathbb{E}^\tau(X)^2 \\
 &= [\mathbb{E}(X) - \mathbb{E}^\tau(X)]^2 \\
 &\geq 0.
 \end{aligned} \tag{30}$$

Based on Eq. (30) and the definition in Eq. (28) and (29), we get

$$\text{Var}^{\tau_{k+1}} \left[ Q_{\tau_{k+1}}^{\pi_{k+1}}(s, a) \right] - \text{Var} \left[ Q_{\tau_{k+1}}^{\pi_{k+1}}(s, a) \right] = \epsilon_1^2. \quad (31)$$

$$\text{Var}^{\tau_k} \left[ Q_{\tau_k}^{\pi_k}(s, a) \right] - \text{Var} \left[ Q_{\tau_k}^{\pi_k}(s, a) \right] = \epsilon_2^2. \quad (32)$$

Then, based on the Cantelli's inequality (one-sided Chebyshev's inequality),

$$\begin{aligned} & P\{Q_{\tau_{k+1}}^{\pi_{k+1}}(s, a) - V_{\tau_{k+1}}^{\pi_{k+1}}(s) \geq 0\} \\ &= P\left\{Q_{\tau_{k+1}}^{\pi_{k+1}}(s, a) - \mathbb{E}_{a \sim \pi_{k+1}}^{\tau_{k+1}} \left[ Q_{\tau_{k+1}}^{\pi_{k+1}}(s, a) \right] \geq 0\right\} \\ &= P\left\{Q_{\tau_{k+1}}^{\pi_{k+1}}(s, a) - \mathbb{E}_{a \sim \pi_{k+1}} \left[ Q_{\tau_{k+1}}^{\pi_{k+1}}(s, a) \right] \geq \epsilon_1\right\} \quad (\text{Eq. (28)}) \\ &\leq \frac{\text{Var} \left[ Q_{\tau_{k+1}}^{\pi_{k+1}}(s, a) \right]}{\text{Var} \left[ Q_{\tau_{k+1}}^{\pi_{k+1}}(s, a) \right] + \epsilon_1^2} \quad (\text{Cantelli's Inequality}) \\ &= \frac{\text{Var} \left[ Q_{\tau_{k+1}}^{\pi_{k+1}}(s, a) \right]}{\text{Var}^{\tau_{k+1}} \left[ Q_{\tau_{k+1}}^{\pi_{k+1}}(s, a) \right]}. \end{aligned} \quad (33)$$

Similarly,

$$P\{Q_{\tau_k}^{\pi_k}(s, a) - V_{\tau_k}^{\pi_k}(s) \geq 0\} \leq \frac{\text{Var} \left[ Q_{\tau_k}^{\pi_k}(s, a) \right]}{\text{Var}^{\tau_k} \left[ Q_{\tau_k}^{\pi_k}(s, a) \right]}. \quad (34)$$

When  $0.5 \leq \tau_k(a|s) \leq \tau_{k+1}(a|s) \leq 1$ , we have  $\text{Var}^{\tau_{k+1}}(X) \geq \text{Var}^{\tau_k}(X) \geq \text{Var}(X) \geq 0$ . Therefore, combining Eq. (33) with (34), Theorem. 4.7 holds.  $\square$

## B. Experimental Details

The vast majority of the hyperparameters in our experiments are consistent with those used in IQL, as summarized in Tab. 3.

The hyperparameters specified for each experiment are described below. Any hyperparameters not explicitly mentioned will default to those shown in Tab. 3.

**For the experiments corresponding to Fig. 1.** We adjusted only the  $\tau = 0.3, 0.6, 0.9$ . All other hyperparameters remained consistent with those listed in Tab. 3.

**For the experiments corresponding to Fig. 2.** We referenced the parameters listed in Tab. 3. In addition, following the suggestions of the authors of the dataset, we subtract 1 from rewards for the AntMaze-v0 datasets.

**For the experiments corresponding to Fig. 3.** We referenced the parameters listed in Tab. 3, but the batch size is modified as 16, 64, 128, 256.

**For the experiments corresponding to Tab. 1 and 2.** We referenced the parameters listed in Tab. 3.

Table 3. Hyperparameters

Hyperparameter	Value	Environment / Network
Hidden Layers	2	All
Layer Width	256	All
Activations	RuLU	All
Learning Rate	3e-4	All
Soft Update	5e-3	All
Training Gradient Steps	1e6	Gym-MuJoCo-v2 & AntMaze-v0 tasks
	2e5	Kitchen-complete-v0 task
	5e5	Kitchen-partial-v0 & Kitchen-mixed-v0 tasks
Evaluation Epochs	10	All
Evaluation Frequency	5e3	All
Random Seed	[0, 2, 4, 6, 8]	All
Batch Size	256	All
	10.0	AntMaze-v0
Inverse Temperature $\frac{1}{\lambda}$	3.0	Gym-MuJoCo-v2
	0.5	Kitchen-v0
Behavior Policy Training Step	1e5	All
	0.9	AntMaze-v0
$\tau$	0.7	Gym-MuJoCo-v2
	0.7	Kitchen-v0
Exponentiated Advantage	$(-\infty, 100]$	All
	0	All Q networks and target-Q networks
Dropout	0	All value networks
	0	Policy networks for AntMaze-v0 and Gym-MoJoCo-v2 tasks
	0.1	Policy networks for Kitchen-v0 tasks